The Journal of Headache and Pain

RESEARCH Open Access

Dysfunctional mesocorticolimbic circuitry in cluster headache

Stefania Ferraro[1,2], Greta Demichelis[3], Jean Paul Medina Carrion[3], Dan Liu[1,2], Benjamin Becker[4,5], Michael Maes[1], Davide Fedeli[3], Giuseppe Ciullo[3,6], Susanna Usai[8], Marina Grisoli[3], Luisa Chiapparini[7], Alberto Cecchini Proietti[8], Luca Giani[9], Anna Nigri[3*] and Massimo Leone[8]

Abstract

Background This study aimed to identify mesocorticolimbic functional abnormalities in cluster headache (CH) patients, disentangling the roles of chronification and affective symptoms.

Methods Using the monetary incentive delay fMRI task to directly engage these pathways, we investigated functional alterations in key regions of this network in chronic ($n=23$) and episodic CH patients ($n=49$) compared to a control group ($n=32$). After processing the fMRI data, we extracted beta values from selected regions and for contrasts of interest and entered them into logistic regression models adjusted for potential confounders (such as depressive and anxiety symptoms and smoking habit) to test their association with the diagnoses (chronic CH and control subjects, episodic CH and control subjects).

Results Results showed that chronic CH patients exhibited reduced ventral tegmental area (VTA) activity and a tendency towards significance ($p=0.056$) for an increased medial prefrontal cortex (mPFC) responsiveness during reward anticipation, alongside a significant decrease in mPFC activity during reward outcomes. Episodic patients displayed abnormal mPFC activity across both reward phases, but coupled with intact VTA responses. Importantly, these functional abnormalities were not correlated to depressive and anxiety symptoms and smoking habits.

Conclusions These findings suggest that chronic CH patients experience an imbalance in the VTA-mPFC pathway, while episodic patients may show early signs of this emerging dysfunction. Moreover, the observed reward processing alterations seem distinct from those associated with affective disorders, possibly highlighting unique mechanisms underlying the pathophysiology of CH.

Keywords Chronic cluster headache, Episodic cluster headache, fMRI , Monetary incentive delay task, Mesocorticolimbic system, Ventral tegmental area, Medial prefrontal cortex, Nucleus accumbens

*Correspondence:
Anna Nigri
anna.nigri@istituto-besta.it
[1]Sichuan Provincial Center for Mental Health, Sichuan Provincial People's Hospital, School of Medicine, University of Electronic Science and Technology of China, Chengdu 610072, China
[2]School of Life Science and Technology, University of Electronic Science and Technology of China, Chengdu, China
[3]Neuroradiology Unit, Fondazione IRCCS Istituto Neurologico 'Carlo Besta', Milan, Italy
[4]State Key Laboratory of Brain and Cognitive Sciences, The University of Hong Kong, Pokfulam, Hong Kong
[5]Department of Psychology, The University of Hong Kong, Pokfulam, Hong Kong
[6]Department of Medicine and Surgery, University of Parma, Parma, Italy
[7]Radiodiagnostic and Neuroadiology Unit, Fodazione IRCCS Policlinico San Matteo, Pavia, Italy
[8]Department of Neurology and Headache Centre, Fondazione IRCCS Istituto Neurologico 'Carlo Besta', Milan, Italy
[9]Neurological Rehabilitation Unit of Milano Institute, Istituti Clinici Scientifici Maugeri IRCCS, Milan, Italy

Introduction

Although the etiology of cluster headache (CH) is not yet fully elucidated, a central origin has been hypothesized, with the hypothalamus as a potential key structure in the pathogenesis of this condition [23]. However, several works have also highlighted neuroplastic changes in a broader set of brain regions [2, 14, 21, 42, 53] with recent evidence suggesting a dysfunction in the functional connectivity among the salience, executive, and default mode network, possibly indicating reduced flexibility in switching between internally and externally directed brain states [1]. In this framework, our group has recently shown that patients with the chronic form of CH present resting-state functional alterations and anatomical abnormalities of the mesocorticolimbic system [16, 17].

Clinical research has consistently demonstrated abnormalities in this network in various chronic pain conditions [56], identifying it as a key player in the transition from acute to chronic pain [6, 60] and indicating that progressive dysregulations in reward processing and motivational/emotional deficits could play a crucial role in this process. A recent theory proposes that the corticolimbic system plays a crucial role in preventing the development of chronic pain by regulating emotional responses to aversive stimuli. In individuals with greater susceptibility, this regulatory control would be lost, resulting in a more intense emotional response to pain that, through a learning process involving the corticolimbic system, would lead to neural maladaptation, eventually resulting in the reverberation and amplification of pain [59]. In line with this, the high prevalence of psychiatric comorbidities in chronic pain - such as depression, anxiety, and addiction - along with evidence indicating that mesocorticolimbic dysregulations are core transdiagnostic pathogenetic mechanisms across multiple domains and psychiatric disorders [9, 15, 54], suggest that abnormalities in this network are related to the transition into chronic pain and/or to psychiatric co-morbidity. However, the relationship among the development and maintenance of chronic pain, the accompanying psychiatric/affective symptoms, and the specific relationships with alterations in the mesocorticolimbic/reward system remain controversial.

Trying to overcome the limitations of our previous works [16, 17], in this study, we took a decisive step in studying the mesocorticolimbic system in the context of CH by investigating distinct groups of patients (chronic and episodic) alongside healthy controls and employing the Monetary Incentive Delay (MID) [31] functional magnetic resonance imaging (fMRI) task to probe the mesocorticolimbic system directly. The MID task, a well-established paradigm in neuropsychiatric research [29], effectively elicits reward-related cognitive processes allowing solid conclusions about alterations of the dopaminergic system, known to be compromised also in CH condition [12, 13].

We specifically assessed whether the ventral tegmental area (VTA), the nucleus accumbens (Nacc), and the medial prefrontal cortex (mPFC), key regions of the mesocorticolimbic/dopaminergic system, are functionally impaired in the chronic form (cCH) and/or in the episodic form (eCH) of CH, with a focus on isolating the effects of chronification. Furthermore, we assessed the relationship between these functional abnormalities and affective symptoms, as well as other clinical factors, such as smoking, to assess their influence on the observed abnormalities.

Methods

Participants

A total of 85 CH patients were consecutively recruited from those who were hospitalized to treat recurrent attacks or being treated at outpatient clinics. All patients were diagnosed by experienced neurologists (M.L., A.P., L.G.) according to the criteria of the International Classification of Headache Disorders, 3rd edition (ICHD-3) [44]. Exclusion criteria were the following: concomitant diagnosis of other primary or secondary headache disorders, cardiovascular disease, diabetes mellitus, hypertension, a history of psychiatric and other neurological conditions, and MRI contraindications. Moreover, the occurrence of a CH attack during the MRI session was an additional key exclusion criterion. After discarding 2 patients because they experienced a CH attack during the MRI session, 2 patients for excessive head movements during fMRI (see next paragraph), and 9 patients for technical problems during fMRI acquisitions, the final sample comprised a total of 72 CH patients [23 cCH, 29eCH in-bout (eCHin), 20 eCH out-of-bout (eCHout)], including 11 females and 61 males (mean age: 44 ± 10.9 years; age range: 22–71 years; see Table 1 for details). A total of 32 healthy participants (CTRL) (5 females, 27 males; mean age 40 ± 11.4 years; age range: 20–68 years) who reported no history of primary headache, chronic pain, or neurological or psychiatric disorders were recruited as controls. Information on the patient's medical history, ongoing medications, and smoking habits was collected during the clinical examination. Before MRI acquisition, all the participants completed the Beck Depression Inventory (BDI-II) [7] and the State-Trait Anxiety Inventory (STAI-S and STAI-T) [57]. CH patients rated the level of headache pain on a 10-cm visual analogue scale (VAS) (0 = no pain; 10 = worst pain imaginable) before and after the MRI. Only one cCH patient reported a pain level of 4 before the MRI session and 5 afterward, but the pain was not defined as a CH attack. The study was approved by the local ethics committee, and written informed consent was obtained from each participant.

Table 1 Demographic and clinical characteristics of the participants and related statistics. *Missing values. Abbreviations: cCH, chronic cluster headache; eCHin, episodic cluster headache patients in-bout; eCHout, episodic cluster headache patients out-of-bout; CTRL, control subjects; Pts, patients; VAS, visual analogue scale (0–10); BDI, Beck Depression Inventory; STAI, State-Trait Anxiety Inventory; M, mean; SD, standard deviation

					Between-group statistics					
	cCH	**eCHin**	**eCHout**	**CTRL**	**cCH vs. CTRL**		**eCH vs. CTRL**		**cCH vs. eCHin vs. eCHout**	
Participants	23	29	20	32	-	-	-	-	-	-
Age (ys; M ± SD)	44 ± 10.2	47 ± 10.9	41 ± 10.2	40 ± 11.4	T(53)= -1.58	$p = 0.120$	T(79)= -1.90	$p = 0.061$	F(2,59) = 1.36	$p = 0.264$
Males/Females	17/6	27/2	17/3	27/5	X2(1,55) = 0.91	$p = 0.339$	X2(1,81) = 0.53	$p = 0.468$	$X^2(2) = 3.65$	$p = 0.161$
BDI scores	12 ± 9.5	12 ± 8.2	8 ± 6.1	5 ± 4.8	U = 120.5	$p = 0.004$	U = 286.5	$p = 0.001$	F(2.58) = 1.13	$p = 0.330$
STAI-S (State anxiety)	50 ± 11.0	53 ± 8.8	48 ± 10.5	48 ± 9.5	U = 208	$p = 0.492$	U = 432.5	$p = 0.183$	F(2,59) = 1.36	$p = 0.264$
STAI-T (Tract anxiety)	47 ± 7.8	50 ± 9.7	52 ± 10.7	45 ± 8.3	U = 191	$p = 0.275$	U = 334	$p = 0.010$	F(2, 59) = 1.14	$p = 0.327$
Smokers/No smokers	15/7 *	20/9	17/3	12/19 *	X2(1,53) = 4.47	$p = 0.034$	X2(1,80) = 10.84	$p < 0.001$	$X^2(2) = 1.97$	$p = 0.374$
Cigarettes per day (Median, range)	8, 0–60	10, 0–40	15, 0–40	0, 0–20	U = 199	$p = 0.015$	U = 350	$p < 0.001$	F(2,68) = 0.29	$p = 0.749$
Right, left, shifting CH attacks	11,6,6	13,15,1	8,12,0	-	-	-	-	-	$X^2(2) = 12.66$	$p = 0.013$
Daily attacks (Median, range)	2.0, 0.3-6	1.5, 0.15-5	-	-	-	-	-	-	F(1,49) = 0.03	$p = 0.853$
Years of disease (Median, range)	-	10, 2–27	13.5, 2–29	-	-	-	-	-	F(1,47) = 0.87	$p = 0.357$
Years of chronic disease (Median, range)	3, 1–23	-	-	-	-	-	-	-	-	-
Pts under Lithium	7	3	1	-	-	-	-	-	$X^2(2) = 5.25$	$p = 0.063$
Pts under Verapamil or Corticosteroids	5	2	4	-	-	-	-	-	$X^2(2) = 2.66$	$p = 0.264$
VAS before MRI (Median, range)	0, 0–4	0, 0–0	0, 0–0	-	-	-	-	-	H(2) = 2.13	$p = 0.345$
VAS after MRI (Median, range)	0, 0–5	0, 0–0	0, 0–0	-	-	-	-	-	H(2) = 2.13	$p = 0.345$

Descriptive statistics of demographic, clinical, and behavioral data

Differences between groups (cCH vs. CTRL and eCH vs. CTRL) for demographic (age, sex) and clinical (BDI and STAI scores, number of active smokers, and number of cigarettes smoked per day) variables were tested. Moreover, for CH patients, differences among diagnostic groups (i.e., cCH, eCHin, and eCHout) for clinical variables (BDI and STAI scores, number of active smokers, number of cigarettes smoked per day, lateralization of attacks, number of attacks per day, years of illness, number of patients on lithium and verapamil/corticosteroid therapy, VAS before and after MRI) were evaluated. For this purpose, after assessing the normality of data distribution and the homogeneity of variance, where necessary, parametric (T-test or ANOVA) or non-parametric (Mann-Whitney test, Chi-square test, Kruskal-Wallis test) statistics were implemented in JASP (v0.18.3.0). The results were considered significant for $p < 0.05$.

MRI assessments

All the participants were scanned with a 3T magnetic resonance imaging (MRI) system (Achieva, Philips Healthcare BV, Best, NL) using a 32-channel head coil. As part of the MRI protocol, high-resolution structural 3D T1-weighted (T1w) image (TR = 9.86 ms, TE = 4.59 ms, FOV = 240 × 240 mm, voxel size = 1 mm^3, flip angle = 8∘, 185 sagittal slices) and T2* 2Dmulti-slice echo-planar imaging (EPI) to collect fMRI data (TR = 2000 ms, TE = 30 ms, FOV = 240 × 240 mm, voxel size = 2.5 mm^3, flip angle = 8∘, 355 volumes, 50 axial slices with 10% gap acquired in ascending order, 3 dummy volumes) were acquired in each participant. Expert neuroradiologists visually inspected all morphological images to exclude apparent brain abnormalities or artifacts affecting the quality of the exam.

Monetary incentive delay (MID) task

Before scanning, participants received detailed instructions on the MID task, performed a 2-minute training session on a laptop computer, and were tested to ensure they fully understood the task. Participants were presented with 2 runs of the MID task, implemented in Eprime (v.3.0.3.31), each one comprising a total of 96 trials. At the beginning of each trial, participants were shown a cue (duration: 2000 ms) indicating whether they

were starting a trial that would potentially lead to a gain (a circle to potentially gain5€, 1€, 0€) or a loss (a square for potentially losing 5€, 1€, 0€). The cue was accompanied by the display of the amount of money the participants could gain or lose in order to reduce learning processes with respect to the presentation of the geometric shape alone. Note that for the purposes of data analyses, gain and loss trials of 0€ were considered control trials. Next, after the presentation of a fixation cross (duration: 2000 ms to 4480 ms), participants were shown a target (triangle, duration: 1000 ms) to which they had to respond as quickly as possible using a response box to win money (in the case of gain trials) or to avoid losing money (in the case of loss trials). If the participants responded in the predetermined time window, the trial was "hit"; otherwise, it was considered "miss". The time window within which the subject had to respond was automatically calculated by an algorithm that readjusted itself for each trial based on the subject's performance to keep the success rate around 66%. Then, the participants received feedback (duration: 2000 ms) on the amount of money won, if the trial was "hit" during the gain trials, or lost if the trial was "missed" during the loss trials. In order not to encourage gambling, and as clarified with each participant at the beginning of the study, the money won was not paid out. Reaction times (RTs) and accuracy rates were collected during the execution of the MID tasks.

Reaction times and accuracy rates during the MID task

For RTs, after discarding all the values below 100 ms (considered anticipated RTs), the median values were calculated for each subject and each type of trial (gain trials, loss trials, and control trials). These values were entered into a repeated measures ANOVA to assess the effects of the within-subject factor 'trial' (gain, loss, control) and the between-subjects factor 'group' (cCH, eCH, CTRL) on RTs.

The same procedure used for RTs was applied to assess the effects of the within-subject factor 'trial' and the between-subjects factor 'group' on accuracy rates.

To exclude possible differences in RTs and accuracy rates between the eCHin and eCHout groups, we repeated the above analyses employing the data from cCH, eCHin, eCHout, and CTRL as between-subjects factor 'group'.

For all the statistics, the results were considered significant for $p < 0.05$. All the statistical analyses were conducted using JASP (v.0.17.1.0) (https://jasp-stats.org).

Regions of interest

To investigate the mesocorticolimbic activity, we selected the following regions of interest (ROIs): the bilateral VTA, Nacc, and mPFC. Nacc and VTA ROIs were extracted from a recent probabilistic atlas [48], while the bilateral mPFC ROI was built as a 10 mm sphere centered in MNI coordinate [± 4 50 3], as already employed in Martucci et al. [35]. All the ROIs were resampled to match the fMRI data resolution.

Analyses of fMRI data

Data preprocessing and processing were performed with SPM12 (Wellcome Department of Imaging Neuroscience, University College, London, UK; http://www.fil.ion.ucl.ac.uk/spm) running on MATLAB R2022a (The Mathworks, Inc.). For each participant, volumes of both fMRI scans were slice-timing corrected, spatially realigned to the first volume of the first functional run, and un-warped to correct for between-scan motion. The T1-weighted image was segmented and spatially normalized to the Montreal Neurological Institute (MNI) space, and the produced parameters were then applied to the T1-w realigned fMRI data for normalization. All functional volumes were then spatially smoothed with a 6 mm full-width half-maximum (FWHM) Gaussian kernel. Motion parameters were used as predictors of no interest in the subsequent statistical analysis (see below), and framewise displacement (FD) [50] was calculated from realignment parameters, with a threshold of 1 employed to determine the number of outliers volumes. If this number exceeded 5% of the scan's total volumes, the whole scan was discarded. This leads to the exclusion of 2 CH patients and to the exclusion of 1 single run in 9 CH and 2 CTRL participants. For each participant, the preprocessed functional data were entered into a first-level analysis using general linear models (GLMs). In the first-level analyses, 4 regressors to identify regions activated by gain and loss anticipation processes (evoked by the presentation of the cue), as well as during "hit" and "miss" outcomes (evoked by the presentation of the feedback) were built as done in previous studies [30, 35]. The regressors were: 1) GainAnt: gain anticipation (cue with + 5€) versus control anticipation (cue with 0€); 2) LossAnt: loss anticipation (cue with − 5€) versus control anticipation (cue with 0€); 3) GainOut: gain hits (feedback with + 5€ or + 1€ outcome) versus gain misses (feedback with 0€) during the outcome phase; 4) NoLossOut: loss hits (feedback with 0€ outcome) versus loss misses (feed-back with − 5€ or -1€ outcome) during the outcome phase. In line with previous studies [27, 35], we did not include the 1€ trials in the GainAnt, and LossAnt contrasts because robust responses during anticipation are present for larger rewards in the NAcc, mPFC, and midbrain areas [30]. However, for the outcome phase, we included the beta values for both outcomes (5€ and 1€) to maximize statistical power. Indeed, for each type of condition, we had 32 trials (16 per run), with an estimated 66.7%success rate ('hit'), which needed to be compared

to the negative outcome ('miss' in about 33.3% of cases). Relying solely on the 5€ condition would have obviously resulted in a limited number of 'missed' trials (we anticipated 22 'hits' and only 10 'misses' for each condition). Therefore, we decided to use the beta values from both outcomes, thus exploiting the maximum statistical power available. Group differences were tested employing the average beta values extracted from each participant (for each ROI and contrast) using the Matlab *getbetas.m* script (https://github.com/scanUCLA/spm12-getBetas) and applying the relevant statistics.

Beta values analyses: binary logistic regression models

The extracted beta values for the selected ROIs were Log-transformed after adding a constant to ensure a minimum value of 1 before being transformed [63]. Based on these values, we identified and excluded the outliers in each group and each contrast by applying the interquartile range method (IQR) [62]. For each of the 4 contrasts, (i.e. GainAnt, LossAnt, GainOut, NoLossOut) the respective Log-beta values of each selected ROI were entered into a 4-block binary logistic regression model to test whether these values could distinguish patients from CTRL participants. In particular, we verified their statistical association with respect to (1) the cCH and CTRL diagnosis and (2) the eCH and CTRL diagnosis. Before this step, we determined the demographic/clinical variables (among the following: age, gender, BDI scores, STAI-S scores, STAI-T scores, and number of cigarettes smoked per day) to be included in the models. Thus, for each statistical association (cCH vs. CTRL and eCH vs. CTRL), we employed univariate logistic regression models (i.e., testing the relationship of the diagnosis with a single predictor at a time), and we retained, to be used in the following 4-block binary logistic regression models, only the predictors with a lax significance of $p < 0.1$, since our aim, in this case, was to identify potential predictor variables and not to test hypotheses [51]. For each 4-block binary logistic regression model, the identified demographic/clinical variables were included in the Null model. To identify the number of predictors to be included in the models, we followed the recommendation to have at least 5 observations for predictor in a logistic regression [61], and if the number of identified predictors exceeded this ratio (1:5), we used additional 4-block binary logistic regression models to test all the identified predictors. Each 4-block binary logistic regression analysis comprised: Model #1, including the selected demo-graphic/clinical variables only; Model #2, including Model #1 as a null model and the beta-transformed values of the VTA; Model #3, including Model #1 and #2 as a null model and the beta-transformed values of the Nacc; Model #4, including model #1, #2 and #3 as a null model and the beta-transformed values of the mPFC. The diagnostic discrimination accuracy of each logistic regression model was evaluated using the area under the receiver characteristic curve (AUC). The odds ratios and corresponding values were also calculated. Due to our robust apriori hypothesis, all the results were considered significant for $p < 0.05$. The use of 4-block binary logistic regression analyses allowed us to adjust for the potential confounding effects of relevant demographic/clinical variables.

As a post-hoc approach, in order to exclude that the differences observed between the eCH group and the CTRL group were driven by a specific subgroup of eCH (eCHin or eCHout), we performed the same binary logistic regression models to verify the statistical association between the Log-beta values and the eCHina and eCHout diagnosis only for the contrasts emerged as significant at the previous step.

Testing linear correlations between beta values and clinical scores

To test for a possible linear correlation of the Log-beta values with the number of headaches per day, Spearman's rho correlation was computed for both cCH and eCHin patients, who were experiencing attacks. Additionally, linear correlations were assessed between the Log- beta values and the years of chronic disease in cCH patients, as well as the year of disease in eCH patients. For all these analyses, only the beta values of the contrasts that emerged as significant in the previous logistic regression analyses were tested.

Results

Demographic, clinical, and behavioral results

For detailed results, see Table 1. The employed statistics showed that the cCH and eCH groups did not differ from the CTRL group in terms of age and sex distribution. Non-parametric t-tests showed that BDI scores for both cCH and eCH groups were significantly different from those of the CTRL group (cCH vs. CTRL: $U = 120.5$, $p = 0.004$; eCH vs. CTRL: $U = 286.5$, $p = 0.001$). In addition, the eCH group, but not the cCH group, showed significantly different STAI-T scale scores compared to the CTRL group ($U = 334$, $p = 0.010$).

Despite the observed differences in BDI and STAI scores, most CH participants reported mild BDI scores, with only a few patients showing severe levels of depression (BDI scores ≥ 30: 1 cCH, 2 eCHin, 0 eCHout) or severe levels of anxiety (scores ≥ 59: STAI-S: 4 cCH, 4 eCHin, 2 eCHout; STAI-T: 2 cCH, 5 eCHin, 3 eCHin). Both cCH and eCH groups also differed significantly from the CTRL group in the number of active smokers (cCH vs. CTRL: $U = 199$, $p = 0.015$; eCH vs. CTRL: $U = 350$, $p < 0.001$). The CH groups (cCH, eCHin, eCHout)

differed in the lateralization of the attacks [$\chi 2(4) = 12.66$, $p = 0.013$] but not in other considered variables.

Reaction times and accuracy rates during the monetary incentive delay task

For the results related to this paragraph, see Tables 2 and Fig. 1. The repeated measures ANOVA on RTs (within-subject factor 'trial': gain, loss, control; between-subjects factor 'group': cCH, eCH, CTRL) showed a significant effect of the factor 'trial' [$F(2,202) = 10.12$, $p < 0.001$]. The post-hoc comparison showed that both Gain and Loss trials were significantly different from the Control trial (Gain vs. Control, t = -3.75, pholm < 0.001; Loss vs. Control, t =-3.68, pholm < 0.001). Across all groups, the RTs during the Control trials (M = 212.6 ms, DS = 28.36 ms) were longer compared to the RTs of both Gain (M = 206.8 ms, SD = 23.49 ms) and Loss trials (M = 207.5 ms, SD = 26.33 ms). No effects were detected for the factor 'group' or for the interaction between the two factors. The same analysis conducted employing the data from cCH, eCHin, eCHout, CTRL as between-subjects factor 'group' showed similar results, with a significant effect of the factor 'trial' [$F(2,200) = 9.17$, $p < 0.001$] and no effects detected for the factor 'group' or for the interaction between the two factors.

The adaptive algorithm was able to target from 62.6 to 70.6% of accuracy rate across all participants and across all the conditions.

The repeated measures ANOVA on accuracy rates (within-subject factor 'trial': gain, loss, control; between-subjects factor 'group': cCH, eCH, CTRL) showed a significant effect of the factor 'trial' [$F(2,202) = 3.34$, $p = 0.037$] and of the between-subject factor 'group' [$F(2,101) = 4.12$, p = < 0.019)] with no significant interactions between them. A closer inspection revealed that the accuracy rate was slightly reduced during Control trials (M = 66%, DS = 11.5%) compared to the Gain and Loss trials (respectively, M = 68%, DS = 7.6%, and M = 69%, DS = 8.2%) with the cCH patients presenting slightly higher accuracy with respect to the other groups. The post-hoc analyses confirmed this observation in cCH patients in respect to the CTRL group (t = 2.82, pholm = 0.017; cCH: M = 70.5%, SD = 11.05%; CTRL: M = 62.56%, SD = 11.40%).

The same analysis conducted employing the data from cCH, eCHin, eCHout, CTRL as between-subjects factor 'group' confirmed the previous results showing significant effects for the within-subject factor 'trial' [$F(2,200) = 4.18$, < 0.017)] and the between-subject factor 'group' [$F(3,100) = 2.83$, p = < 0.042)], with no significant interactions between them.

Table 2 Descriptive statistics and repeated measures ANOVA results (within-subject factor 'trial': gain, loss, control; between-subjects factor 'group': cCH, eCHin, eCHout, CTRL) for reaction times (in ms) and accuracy levels (in percentage) during the MID fMRI task. *Significant p-value ($p < 0.05$). Abbreviations: ANOVA, analyses of variance; cCH, chronic cluster headache patients; eCHin, episodic cluster headache in-bout patients; eCHout, episodic cluster headache out-of-bout patients; CTRL, control subjects; RTs, reaction times

	Descriptive Statistics										Repeated Measures ANOVA		
	GAIN trial				LOSS trial				CONTROL trial				
	cCH	eCHin	eCHout	CTRL	cCH	eCHin	eCHout	CTRL	cCH	eCHin	eCHout	CTRL	Factor 'Trial'	Factor 'Group'	Interaction
RT (ms)													F(2,200) = 9.17, $p < 0.001$*	F(3,100) = 0.40, $p = 0.756$	F(6,200) = 0.70, $p = 0.653$
M	208.6	208.8	204.6	205.1	210.9	210.8	202.9	205.0	213.8	215.5	206.4	213.0			
SD	26.28	30.33	14.61	19.24	35.13	31.95	16.90	17.06	36.32	32.68	16.46	23.92			
Accuracy (%)													F(2,200) = 4.18, $p = 0.017$*	F(3,100) = 2.83, $p = 0.042$*	F(6,200) = 0.73, $p = 0.629$
M	69.8	69.8	67.9	66.7	70.1	70.6	69.1	67.7	70.5	65.1	65.7	62.6			
SD	7.77	7.65	8.43	6.98	8.10	9.56	6.23	8.05	11.05	11.09	11.93	11.40			

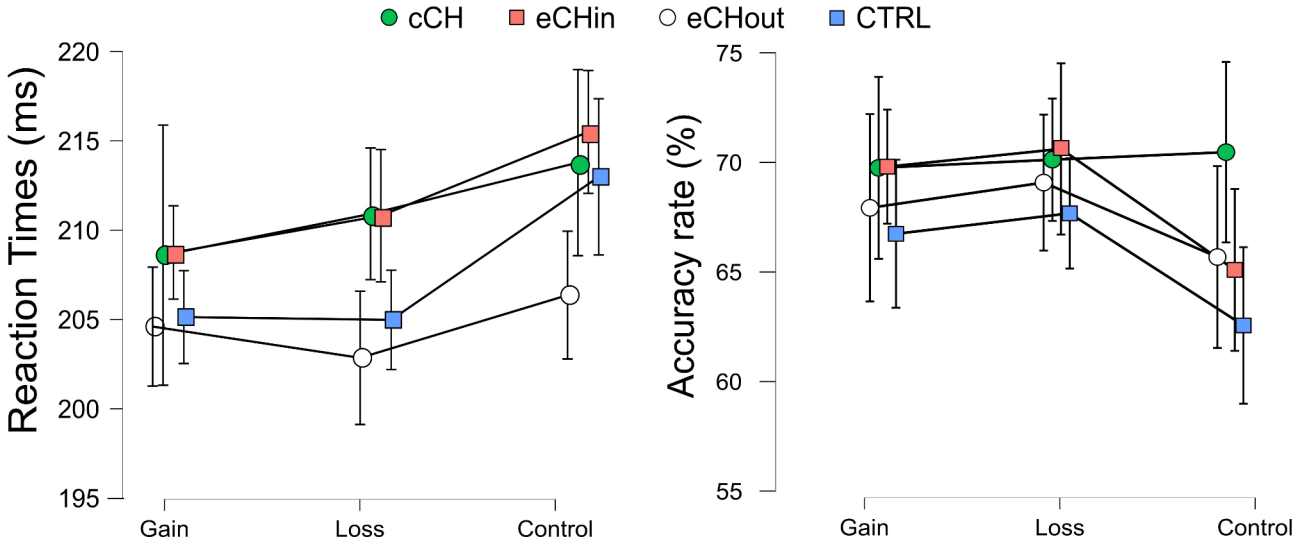

Fig. 1 Median of the reaction times (RTs) expressed in milliseconds and accuracy rates collected during the different conditions (Gain, Loss, and Control) of the MID fMRI task. Abbreviations: cCH, chronic cluster headache; eCHin, episodic cluster headache patients in-bout; eCHout, episodic cluster headache patients out-of-bout; CTRL, control participants

Table 3 Descriptive statistics of Log-beta values extracted from the selected rois [ventral tegmental area (VTA), nucleus accumbens (Nacc), and medial prefrontal cortex (mPFC)]. Abbreviations: cCH, chronic cluster headache; eCH, episodic cluster headache; CTRL, control subjects; M, mean; SD, standard deviation; Min, minimum; Max, maximum.

	VTA			Nacc			mPFC		
GainAnt	**cCH**	**eCH**	**CTRL**	**cCH**	**eCH**	**CTRL**	**cCH**	**eCH**	**CTRL**
# outliers	1	4	0	1	4	0	1	5	1
M	0.746	0.842	0.854	0.868	0.895	0.901	1.943	1.946	1.94
SD	0.178	0.151	0.109	0.096	0.089	0.079	0.012	0.008	0.009
Min	0.437	0.425	0.625	0.668	0.68	0.79	1.921	1.925	1.92
Max	1.081	1.134	1.103	1.02	1.112	1.113	1.963	1.962	1.956
LossAnt									
# outliers	0	1	2	2	3	2	1	4	2
M	0.968	0.967	0.969	0.715	0.708	0.736	1.075	1.076	1.075
SD	0.106	0.101	0.1	0.102	0.105	0.091	0.061	0.055	0.068
Min	0.728	0.709	0.71	0.549	0.461	0.535	0.915	0.951	0.93
Max	1.131	1.162	1.163	0.936	0.926	0.881	1.157	1.182	1.163
GainOut									
# outliers	1	2	2	2	2	0	2	3	2
M	1.396	1.394	1.356	1.345	1.359	1.316	1.146	1.214	1.249
SD	0.128	0.103	0.117	0.081	0.077	0.074	0.184	0.162	0.086
Min	1.127	1.169	1.097	1.152	1.182	1.128	0.86	0.828	1.079
Max	1.688	1.613	1.554	1.47	1.548	1.437	1.442	1.526	1.446
NoLossOut									
# outliers	3	2	2	0	3	2	1	4	1
M	1.257	1.183	1.181	1.142	1.138	1.138	1.369	1.355	1.405
SD	0.12	0.146	0.175	0.112	0.114	0.096	0.1	0.094	0.093
Min	1.044	0.836	0.873	0.894	0.858	0.958	1.147	1.129	1.169
Max	1.513	1.445	1.529	1.379	1.381	1.318	1.521	1.552	1.554

Beta values analyses: logistic regression models

Descriptive statistics for the Log-beta values are reported in Table 3; Fig. 2. Logistic regression results are reported in Tables 4, 5 and 6.

Association with the diagnosis: cCH vs. CTRL

Univariate logistic regression models (see Table 4) showed that among the variables tested (age, gender, BDI, STAI-S, and STAI-T, number of cigarettes smoked per day), BDI scores ($p = 0.001$) and the number of cigarettes

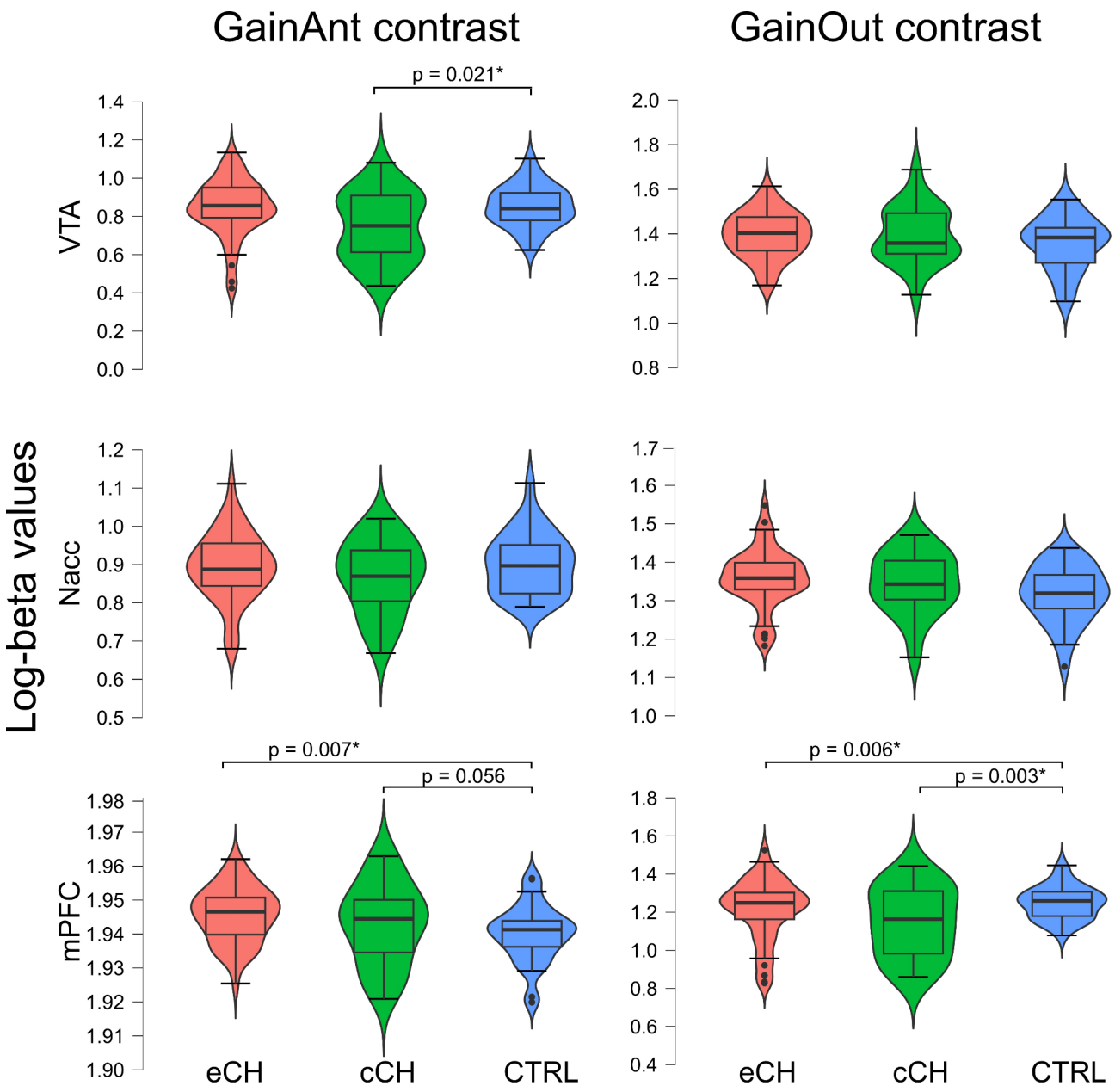

Fig. 2 Log-beta values extracted from the key areas of the mesocorticolimbic system for the anticipation of gain (GainAnt contrast) and the outcome of Gain (GainOut contrast). The reported *p*-values (* significant) were obtained employing binary logistic regression models. See the main text for further details. Abbreviations: VTA, ventral tegmental area; Nacc, nucleus accumbens; mPFC, medial prefrontal cortex; cCH, chronic cluster headache; eCGin, episodic cluster headache patients in-bout; eCHout, episodic cluster headache patients out-of-bout; CTRL, control participants; GainAnt, contrast gain anticipation vs. control anticipation; GainOut, contrast gain hits versus gain misses during the outcome phase

smoked per day ($p = 0.012$) were predictors of the diagnosis based on the chosen arbitrary threshold ($p < 0.1$). In order to retain the 1:5 ratio between predictors in the logistic regression and observations (smallest group cCH = 23 patients), only BDI scores were included in the subsequent 4-block logistic regression models, with the beta-transformed values of the 3 ROIs. For the significant contrasts only, to test the possible confounding effect of cigarettes smoked per day, we performed the same logistic regression models using the number of cigarettes smoked per day instead of the BDI scores.

The 4-block logistic regression models (see Table 5) testing the association with the cCH and CTRL diagnosis showed that Model#1 (with the BDI scores) successfully discriminated between the two groups as expected [$\chi 2(43) = 10.29$, $p = 0.001$, Nagelkerke $R^2 = 0.275$]. Regarding the GainAnt contrast, the cCH and CTRL diagnoses were significantly better predicted by Model #2

Table 4 Univariate binary logistic regression models results. Univariate binary logistic regression models were used to estimate the probability of CH compared to CTRL, using demographic and clinical variables of interest as predictors. To identify potential predictor variables to be used in the 4-block logistic regression models, rather than test hypotheses (Ranganathan et al., 2017), p-values < 0.1 (*) were considered significant. cCH, chronic cluster headache; eCH, episodic cluster headache; CTRL, control participants, BDI, Beck depression inventory; STAI, State-Trait anxiety inventory

	df	ΔX^2	*p*	Nagelkerke R^2	df	ΔX^2	*p*	Nagelkerke R^2
Predictors	**cCH vs. CTRL**				**eCH vs. CTRL**			
Age	53	2.50	0.114	0.06	79	3.63	0.057*	0.059
Sex	53	0.90	0.342	0.022	79	0.52	0.473	0.009
BDI	43	10.29	0.001*	0.275	66	11.75	< 0.001*	0.216
STAI-T	42	0.65	0.419	0.02	66	1.46	0.228	0.029
STAI-S	42	0.74	0.389	0.022	66	5.71	0.017*	0.11
# cigarettes/day	49	6.24	0.012*	0.155	76	16.27	< 0.001*	0.257

comprising the VTA Log-beta values [$\chi2(41) = 5.31$, $p = 0.021$, NagelkerkeR² = 0.168] compared to Model #1. As expected, Model #2 achieved better performance (AUC = 0.81) compared to Model#1 (AUC = 0.76). Model #3 and Model #4 did not improve prediction accuracy compared to the previous models. However, Model #4, comprising the mPFC Log-beta values, showed a tendency towards significance [$\chi2(37) = 3.65$, $p = 0.056$, Nagelkerke R² = 0.132]. The Log-beta values showed that cCH patients presented blunted VTA activity (see Fig. 2; Table 3) and a slightly increased mPFC activity in comparison to CTRL. In regard to the GainOut contrast, only Model #4, comprising the mPFC Log-beta values, predicted significantly better the diagnosis with respect to Model #3 [$\chi2(36) = 8.43$, $p = 0.004$, Nagelkerke R² =0.272] with an amelioration of the AUC (from 0.735 to 0.843). The Log-beta values showed that cCH patients presented reduced mPFC Log-beta values in comparison to CTRL (see Fig. 2; Table 3). For the LossAnt contrast and NoLossOut contrast, no model predicted the diagnosis significantly better than Model #1.

The 4-block logistic regression models using only the number of cigarettes smoked per day as a clinical variable confirmed that the significant results from the previous logistic regression statistics were not confounded by different smoking habits between the investigated groups, as the results remained consistent (see Table 5).

Association with the diagnosis: eCH vs. CTRL

Univariate logistic regression models (see Table 4) indicated that age ($p = 0.057$), BDI scores ($p = 0.001$), STAI-T scores ($p = 0.017$), and the number of cigarettes smoked per day ($p < 0.001$) were predictors of the diagnosis based on the chosen arbitrary threshold ($p < 0.1$).

In order to retain the 1:5 ratio between predictors and observations (smallest group CTRL = 32 participants), age, BDI scores, and STAI-T scores (3 predictors) were included as predictors in the subsequent logistic regression models. As mentioned above, to test the possible confounding effect of cigarettes smoked per day, we performed, for the significant contrasts only, the same logistic regression models using only the number of cigarettes smoked per day in Model #1.

The 4-block logistic regression models (see Table 5) testing the association with the eCH and CTRL diagnosis showed that Model #1, which included age, BDI, and STAI-T scores as predictors, successfully discriminated between the diagnoses [$\chi2(63) = 13.59$, $p = 0.004$, Nagelkerke R² = 0.25]. Regarding the GainAnt contrast, only Model 4, comprising the mPFC Log-beta values, predicted the diagnosis significantly better than Model #3 [$\chi2(51) = 5.87$, $p = 0.015$, Nagelkerke R²= 0.138]. Model #4 achieved better performance (AUC = 0.78) compared to Model #3 (AUC = 0.74). The Log-beta values showed that eCH patients presented increased mPFC Log-beta values in comparison to CTRL (see Fig. 2; Table 3). In regard to the GainOut contrast, Model #4, comprising the mPFC Log-beta values, predicted significantly better the diagnosis with respect to Model #3 [$\chi2(55) = 6.54$, $p = 0.011$, Nagelkerke R² = 0.153]. Also in this case, there was an amelioration of the AUC (from 0.78 to 0.84). Log-beta values showed that eCH patients presented blunted mPFC Log-beta values in comparison to CTRL (see Fig. 2; Table 3). In the LossAnt contrast, we found that adding Model #3 comprising the Nacc Log-beta values, predicted significantly better the diagnosis with respect to Model #2. However, we did not consider this result as significant since the confidence interval of the coefficient b (see Table 6) included the zero value, thus indicating that it is not possible to rule out the null hypothesis of no effect. For the NoLossOut contrasts, no model predicted the diagnosis significantly better than Model #1. The 4-block logistic regression models with only the number of cigarettes smoked per day as a clinical variable confirmed the significant results observed in the previous logistic regression analysis (see Table 5).

Overall, logistic regression analyses indicate that during gain anticipation (GainAnt) cCH patients showed an attenuated VTA response associated with an increase (although not reaching full significance) in mPFC activity,

Table 5 4-block binary logistic regression model results. For each contrast, a 4-block logistic regression model estimated the probability of CH compared to CTRL using the Log-beta values as predictors. We computed the area under the curve, sensitivity, specificity, and precision for the model with demographic/clinical predictors only, the model with demographic/clinical predictors and VTA Log-beta values, the model with demographic/clinical predictors, VTA, and NAcc Log-beta values, and the model with demographic/clinical predictors, VTA, NAcc, and mPFC Log-beta values. * Significant p-value ($p < 0.05$). Abbreviations: cCH, chronic cluster headache; eCH, episodic cluster headache; CTRL, control participants; BDI, Beck depression inventory; STAI-T, state anxiety Inventory - Trait; VTA, ventral tegmental area; Nacc, nucleus accumbens; mPFC, medial prefrontal cortex; AUC, area under the curve; sens., sensitivity; spec., specificity; prec., precision

	cCH vs. CTRL								
CONTRAST	**Model**	**df**	**X^2**	***p***	**Nagelkerke R^2**	**AUC**	**Sens**	**Spec**	**Prec**
	(BDI)	43	10.29	0.001*	0.275	0.756	0.579	0.731	0.611
GainAnt	M0 (BDI) + VTA	41	5.31	0.021*	0.168	0.812	0.778	0.923	0.875
	M0 (BDI, VTA) + Nacc	39	0.23	0.633	0.008	0.826	0.824	0.923	0.875
	M0 (BDI, VTA, Nacc) + mPFC	37	3.65	0.056	0.132	0.864	0.706	0.92	0.857
LossAnt	M0 (BDI) + VTA	40	0.24	0.625	0.008	0.752	0.579	0.792	0.688
	M0 (BDI, VTA) + Nacc	37	0.55	0.457	0.02	0.809	0.556	0.87	0.769
	M0 (BDI, VTA, Nacc) + mPFC	35	0.29	0.593	0.011	0.826	0.667	0.818	0.75
GainOut	M0 (BDI) + VTA	39	0.07	0.79	0.002	0.769	0.556	0.75	0.625
	M0 (BDI, VTA) + Nacc	37	0.82	0.367	0.029	0.735	0.412	0.833	0.636
	M0 (BDI, VTA, Nacc) + mPFC	36	8.43	0.004*	0.272	0.843	0.588	0.792	0.667
NoLossOut	M0 (BDI) + VTA	38	2.03	0.154	0.07	0.721	0.529	0.875	0.75
	M0 (BDI, VTA) + Nacc	35	0.25	0.614	0.009	0.711	0.529	0.818	0.692
	M0 (BDI, VTA, Nacc) + mPFC	33	3.30	0.069	0.124	0.815	0.688	0.818	0.733
	ADDITIONAL MODEL (smoke)	49	6.24	0.012*	0.155	0.688	0.409	0.862	0.692
GainAnt	M0 (smoke) + VTA	47	6.00	0.014*	0.16	0.767	0.667	0.828	0.737
	M0 (smoke, VTA) + Nacc	45	0.90	0.343	0.027	0.764	0.65	0.862	0.765
	M0 (smoke, VTA, Nacc) + mPFC	43	7.86	0.005*	0.224	0.832	0.65	0.821	0.722
GainOut	M0 (smoke) + VTA	45	0.72	0.395	0.012	0.711	0.429	0.815	0.643
	M0 (smoke, VTA) + Nacc	43	1.21	0.271	0.035	0.715	0.4	0.852	0.667
	M0 (smoke, VTA, Nacc) + mPFC	42	8.13	0.004*	0.222	0.741	0.5	0.889	0.769
	eCH vs. CTRL								
	(Age, BDI, STAI-T)	63	13.59	0.004	0.25	0.762	0.786	0.56	0.75
GainAnt	M0 (BDI, STAI-T) + VTA	58	0.01	0.943	$1.204 \times 10 - 4$	0.751	0.763	0.6	0.744
	M0 (BDI, STAI-T, VTA) + Nacc	55	0.13	0.716	0.003	0.737	0.778	0.6	0.737
	M0 (BDI, STAI-T, VTA, Nacc) + mPFC	51	5.87	0.015*	0.138	0.779	0.794	0.583	0.73
LossAnt	M0 (BDI, STAI-T) + VTA	59	0.63	0.427	0.015	0.761	0.854	0.565	0.778
	M0 (BDI, STAI-T, VTA) + Nacc	54	2.50	0.114	0.06	0.736	0.842	0.5	0.744
	M0 (BDI, STAI-T, VTA, Nacc) + mPFC	50	0.05	0.819	0.001	0.762	0.833	0.476	0.732
GainOut	M0 (BDI, STAI-T) + VTA	59	0.15	0.696	0.004	0.751	0.8	0.5	0.727
	M0 (BDI, STAI-T, VTA) + Nacc	57	3.01	0.083	0.069	0.784	0.846	0.625	0.786
	M0 (BDI, STAI-T, VTA, Nacc) + mPFC	55	6.54	0.011*	0.153	0.842	0.816	0.708	0.816
NoLossOut	M0 (BDI, STAI-T) + VTA	58	0.35	0.555	0.008	0.762	0.85	0.522	0.756
	M0 (BDI, STAI-T, VTA) + Nacc	52	0.45	0.502	0.011	0.761	0.919	0.571	0.791
	M0 (BDI, STAI-T, VTA, Nacc) + mPFC	50	2.42	0.12	0.061	0.75	0.833	0.476	0.732
	ADDITIONAL MODEL (smoke)	76	16.27	< 0.001*	0.257	0.754	0.694	0.724	0.81
GainAnt	M0 (smoke) + VTA	71	1.58	0.209	0.031	0.758	0.711	0.655	0.762
	M0 (smoke, VTA) + Nacc	68	0.64	0.422	0.013	0.772	0.698	0.759	0.811
	M0 (smoke, VTA, Nacc) + mPFC	64	10.65	0.001*	0.211	0.821	0.805	0.679	0.786
GainOut	M0 (smoke) + VTA	71	0.80	0.37	0.016	0.738	0.745	0.667	0.795
	M0 (smoke, VTA) + Nacc	69	3.00	0.083	0.06	0.779	0.783	0.556	0.75
	M0 (smoke, VTA, Nacc) + mPFC	66	4.74	0.03*	0.097	0.801	0.795	0.593	0.761

Table 6 4-block binary logistic regression model results: parameters value. For each contrast, a 4-block logistic regression model estimated the probability of CH compared to CTRL. Odds ratios (OR) are based on U unit change of the independent variable. ^ U = 100. Abbreviations: cCH, chronic cluster headache; eCH, episodic cluster headache patients; CTRL, control participants; BDI, Beck depression inventory; STAI-T, state anxiety Inventory - Trait; VTA, ventral tegmental area; Nacc, nucleus accumbens; mPFC, medial prefrontal cortex; LB: lower boundary; UB: upper boundary

		b	SE	OR	z	Wald Test	*p*	LB (95% CI)	UB (95% CI)
	cCH vs. CTRL								
GainAnt	(Intercept)	-185.99	106.92	1.681×10^{-81}	-1.74	3.03	0.082	-395.54	23.56
	BDI	0.17	0.06	1.19	2.70	7.28	0.007	0.05	0.29
	VTA	-8.33	4.24	0.92^	-1.97	3.86	0.049	-16.64	-0.03
	Nacc	4.58	6.43	97.18	0.71	0.51	0.477	-8.03	17.18
	mPFC	96.17	55.12	2.616^	1.75	3.04	0.081	-11.87	204.20
LossAnt	(Intercept)	-2.87	7.33	0.06	-0.39	0.15	0.696	-17.23	11.50
	BDI	0.22	0.08	1.25	2.77	7.68	0.006	0.07	0.38
	VTA	-2.56	4.21	0.08	-0.61	0.37	0.543	-10.80	5.69
	Nacc	6.69	4.68	807.04	1.43	2.05	0.153	-2.48	15.87
	mPFC	-3.46	6.45	0.03	-0.54	0.29	0.592	-16.10	9.19
GainOut	(Intercept)	-7.47	8.24	5.707×10^{-4}	-0.91	0.82	0.365	-23.61	8.68
	BDI	0.14	0.07	1.16	2.05	4.22	0.04	0.01	0.28
	VTA	-0.72	3.31	0.49	-0.22	0.05	0.827	-7.21	5.76
	Nacc	16.63	8.16	1.181^	2.04	4.15	0.042	0.63	32.62
	mPFC	-12.38	5.41	0.884^	-2.29	5.23	0.022	-22.99	-1.77
NoLossOut	(Intercept)	0.34	6.92	1.41	0.05	0.00	0.961	-13.23	13.91
	BDI	0.18	0.07	1.20	2.53	6.42	0.011	0.04	0.32
	VTA	3.76	3.04	43.02	1.24	1.53	0.216	-2.20	9.73
	Nacc	4.79	4.06	120.53	1.18	1.39	0.238	-3.17	12.75
	mPFC	-8.73	5.05	0.916^	-1.73	3.00	0.083	-18.62	1.16
	eCH vs. CTRL								
GainAnt	(Intercept)	-199.78	87.27	1.721×10^{-87}	-2.29	5.24	0.022	-370.83	-28.74
	AGE	0.02	0.03	1.02	0.70	0.48	0.486	-0.04	0.08
	BDI	0.12	0.08	1.13	1.56	2.44	0.118	-0.03	0.27
	STAI-T	0.02	0.05	1.02	0.34	0.11	0.737	-0.08	0.11
	VTA	0.01	2.49	1.01	0.00	1.771×10^{-5}	0.997	-4.86	4.88
	Nacc	-0.88	5.12	0.42	-0.17	0.03	0.864	-10.91	9.16
	mPFC	102.12	45.48	2.777^	2.25	5.04	0.025	12.98	191.26
LossAnt	(Intercept)	3.63	6.61	37.88	0.55	0.30	0.582	-9.32	16.59
	AGE	0.01	0.03	1.01	0.25	0.06	0.803	-0.05	0.07
	BDI	0.19	0.08	1.21	2.33	5.44	0.02	0.03	0.35
	STAI-T	-0.01	0.04	0.99	-0.18	0.03	0.859	-0.09	0.08
	VTA	1.28	3.86	3.58	0.33	0.11	0.741	-6.30	8.85
	Nacc	-5.75	3.77	0.00	-1.53	2.33	0.127	-13.14	1.63
	mPFC	-1.30	5.68	0.27	-0.23	0.05	0.82	-12.43	9.84
GainOut	(Intercept)	-16.77	7.53	5.214×10^{-8}	-2.23	4.95	0.026	-31.54	-2.00
	AGE	0.02	0.03	1.02	0.71	0.50	0.48	-0.04	0.08
	BDI	0.20	0.08	1.22	2.57	6.63	0.01	0.05	0.35
	STAI-T	-0.01	0.05	0.99	-0.22	0.05	0.826	-0.10	0.08
	VTA	3.07	3.50	21.56	0.88	0.77	0.38	-3.79	9.93
	Nacc	15.93	6.23	1.173^	2.56	6.55	0.011	3.73	28.14
	mPFC	-8.22	3.56	0.921^	-2.31	5.33	0.021	-15.20	-1.24
NoLossOut	(Intercept)	2.27	5.81	9.68	0.39	0.15	0.696	-9.12	13.66
	AGE	0.04	0.03	1.04	1.29	1.66	0.198	-0.02	0.10
	BDI	0.11	0.07	1.12	1.62	2.62	0.105	-0.02	0.25
	STAI-T	0.02	0.05	1.02	0.39	0.15	0.694	-0.07	0.11
	VTA	-1.27	2.26	0.28	-0.56	0.32	0.574	-5.71	3.16
	Nacc	3.92	3.20	50.16	1.22	1.50	0.221	-2.36	10.19
	mPFC	-5.80	3.88	0.00	-1.50	2.24	0.135	-13.39	1.80

Table 7 As post-hoc, we verified whether the observed differences between the eCH and CTRL groups were driven by a subgroup of the eCH patients (i.e., eCHin or eCHout). To this aim, we employed 3-block binary logistic regression models -only for the significant contrasts obtained from the logistic regression testing the differences between the eCH and CTRL groups- to estimate the probability of eCHin compared to eCHout using the Log-beta values as predictors. Since no differences were detected for demographic, clinical, and psychometric data except for a different lateralization of the headache attacks among the different CH groups, we did not include in these logistic regression models any additional variables. Abbreviations: eCHin, episodic cluster headache in-bout; eCHout, episodic cluster headache out-of-bout; VTA, ventral tegmental area; Nacc, nucleus accumbens; mPFC, medial prefrontal cortex; AUC, area under the curve; sens., sensitivity; spec., specificity; prec., precision

	eCHin vs. eCHout								
CONTRAST	**Model**	**df**	**X^2**	***p***	**Nagelkerke R^2**	**AUC**	**Sens**	**Spec**	**Prec**
GainAnt	M0 (VTA)	43	0.52	0.472	0.015	0.561	0.923	0.105	0.585
	M0 (VTA) + Nacc	40	0.01	0.923	0.000	0.535	0.917	0.053	0.550
	M0 (VTA, Nacc) + mPFC	37	1.75	0.186	0.056	0.593	0.773	0.526	0.654
GainOut	M0 (VTA)	45	0.13	0.716	0.004	0.575	1.000	0.000	0.596
	M0 (VTA) + Nacc	43	0.72	0.396	0.021	0.571	0.926	0.105	0.595
	M0 (VTA, Nacc) + mPFC	40	0.01	0.910	0.000	0.562	0.923	0.222	0.632

Table 8 Correlations of the Log-beta values extracted from the rois in the ventral tegmental area (VTA), nucleus accumbens (Nacc), and medial prefrontal cortex (mPFC) with years of chronic disease (in cCH patients), years of disease (in eCH patients), number of daily attacks (in cCH and eCH patients) at the time of scanning. Abbreviations: Ys, years; cCH, chronic cluster headache; eCHin, episodic cluster headache in-bout patients; VTA, ventral tegmental area; Nacc, nucleus accumbens; mPFC, medial prefrontal cortex; n.a, not applicable

	cCH (ys of chronic disease)		**eCH (ys of disease)**		**# attacks/day (cCH, eCHin)**	
	ρ	***p*-value**	**ρ**	***p*-value**	**ρ**	***p*-value**
GAINant						
VTA	0.008	0.972	n.a.	n.a.	0.145	0.33
Nacc	n.a.	n.a.	n.a.	n.a.	n.a.	n.a.
mPFC	n.a.	n.a.	-0.25	0.101	-0.141	0.351
GAINout						
VTA	n.a.	n.a.	n.a.	n.a.	n.a.	n.a.
Nacc	n.a.	n.a.	n.a.	n.a.	n.a.	n.a.
mPFC	-0.139	0.548	-0.08	0.613	0.272	0.065

whereas eCH patients showed only a robust increase in mPFC responsiveness. In contrast, during the gain outcome phase (GainOut), both cCH and eCH patients showed a robust decrease in mPFC activity. These results appear to be independent of the confounding effects of the considered demographic/clinical variables.

Association with the diagnosis: eCHin vs. eCHout.

The logistic regression models (see Table 7), which tested the association between Log-beta values and the diagnoses of eCHin and eCHout–considering only the significant contrasts (GainAnt and GainOut) of the previous logistic regression models testing the association for eCH and CTRL diagnosis–revealed that neither the GainAnt nor the GainOut contrasts were able to predict the diagnosis. Importantly since we did not find any differences for age, sex distribution, smoking habits and psychometric measures, except for the headache attacks lateralization among the CH patients, we did not use any of these variables in the logistic regression models.

Testing linear correlations between Log-transformed beta values and clinical scores

No significant correlations were observed between the Log-beta values of the significant logistic regression models and the number of years of chronic disease in the cCH patients, duration of the disease in the eCH sample, nor with the number of daily headache attacks (in cCH and eCHin patients) (see Table 8).

Discussion

Employing the MID task to directly engage the mesocorticolimbic dopaminergic pathways [31], we investigated functional alterations of key regions in this network (i.e., VTA, Nacc, and mPFC) during different reward processing stages (i.e., anticipation and outcome) in comparably large groups of chronic ($n = 23$) and episodic CH patients ($n = 49$) compared with a control group ($n = 32$).

Through the application of robust statistical methods to control for potential confounding variables, we identified distinct and shared neurophysiological dysfunctions during reward processing in cCH and eCH

patients. Specifically, cCH patients showed blunted VTA activity associated with increased mPFC responsiveness (although the latter did not reach full statistical significance) during reward anticipation (GainAnt contrast), while they showed a marked decrease in mPFC activity during the reward outcome phase. In a distinctive manner, eCH patients displayed an increased mPFC activity during reward anticipation and reduced mPFC activity during reward outcome but in the context of intact VTA responses. Crucially, these functional abnormalities were observed by controlling for depressive and anxiety symptoms as measured by the BDI and STAI scales as well as the smoking habits. This indicates that these alterations are associated with CH pathophysiology rather than to the associated affective symptoms. Importantly, the observed differences between the eCH and CTRL groups were not driven by the specific phases of the investigated eCH patients (eCH in-bout or out-of bout), thus indicating stable functional abnormalities in the mesocorticolimbic circuits in eCH patients.

From a clinical perspective, two aspects of the neural responses to reward anticipation in the MID task are particularly relevant: their relationship to the dopaminergic activity and their association with anhedonia and impaired motivation in neuropsychiatric disorders. Firstly, abnormal fMRI mesocorticolimbic responses to the MID task are thought to be related to dopaminergic dysregulation. In this regard, research indicates that the anticipation phase is characterized by a surge in dopamine levels [55], and it is sensitive to the depletion of dopamine precursors [8] and to the effects of dopamine reuptake inhibitors [28]. Our findings of blunted VTA activity during the reward anticipation thus may reflect an abnormal dopaminergic state in cCH patients. This interpretation also aligns with the well-established observation that chronic pain patients exhibit a hyperdopaminergic state [58] and by a biochemical study showing that cCH patients present abnormal tyrosine metabolism [13]. Secondly, reduced neural activity during reward anticipation has been associated with impaired motivation in neuropsychiatric conditions where the MID task has been widely used [9, 29]. This is particularly important because mesocorticolimbic abnormalities in chronic pain patients are thought to mediate comorbidity with affective symptoms. Recent conceptualizations highlight that dysfunctional emotional salience signals play a critical step in the chronification of pain [60]. However, the relationships among mesocorticolimbic abnormalities, affective symptoms, and chronic pain remain empirically unclear, and few human studies have directly evaluated this association. Kim et al. [26], investigating both fibromyalgia and chronic low back pain with the MID fMRI task, have shown that blunted responses in the striatum during gain anticipation were correlated with anhedonia and depression scores. Similarly, a more recent study showed that patients suffering from non-specific back pain present blunted activity in the ventral striatum during reward anticipation [5]. Differently, Martucci et al. [35], investigating only fibromyalgia patients, showed a decreased response in the mPFC during the anticipation phase but no abnormalities in the VTA and in the Nacc [35]. Notably, in this case, the observed alterations were not linked to depression or anxiety scores. The replication of this study in another sample of fibromyalgia patients further reinforced this observation [47]. Interestingly, the MID task was also used to study episodic migraineurs showing, at a whole-brain level, altered neural processing of the reward outcome [32]. Despite the interesting finding, this research did not report results at the level of mesocorticolimbic ROIs and did not investigate the possible link with emotional disorders, thus preventing a direct comparison with our study. As expected, given the well-documented association between chronic pain and affective comorbidities, CH patients also have a relatively high prevalence (over 30% of cases) of moderate-to-severe anxiety or depression [26]. Given these findings and the above considerations, our study necessarily accounted for the high prevalence of anxiety and depression among CH patients to determine whether the observed results were influenced by these affective symptoms.

Although in our study both cCH and eCH patients presented higher BDI scores than healthy participants, and eCH patients also showed higher STAI-T scores, our results indicate that the observed mesocorticolimbic abnormalities were not related to symptoms of depression and anxiety. This observation does not support the hypothesis that abnormalities in affective processing drive the abnormal mesocorticolimbic responses. Instead, robust statistical analyses (i.e., logistic regression models) incorporating relevant affective scores (BDI and/or STAI) suggest that these mesocorticolimbic alterations are intrinsic to the pathophysiology of CH.

As a crucial region of the mesocorticolimbic system, the VTA projects multiple and complex dopaminergic pathways to the mPFC [34, 49], regulating executive functions [46], and to the nucleus accumbens, regulating motivated behavior and reward-driven learning [40]. Considering the complexity of the dopaminergic system, the co-occurring abnormal signal of the VTA and mPFC in cCH associated with an apparent absence of Nacc dysfunction might indicate a specific involvement of the VTA-mPFC pathways. Although the VTA's role in the pathophysiology of CH remains uncertain and often underestimated, its critical involvement in the chronic form of CH is well documented. This is corroborated by our findings showing marked dysregulation of VTA activity in cCH patients, as well as by its activation during CH

attacks [36, 38] and by empirical evidence that VTA-DBS can control the frequency and severity of attacks [3, 11], probably by inducing a restoration of the abnormal VTA dopaminergic activity.

Although in the context of CH, mPFC has not been given special attention, it is considered a critical region in chronic pain conditions. On the one hand, it is involved in processing multiple aspects of pain, such as sensory [37], cognitive [41], and emotional [19] dimensions. On the other hand, it exhibits important neuroplastic changes in chronic pain conditions [4, 39] with a recent animal study showing that dopaminergic inputs from the VTA modulate mPFC neuronal activity, potentiating the activity of periaqueductal gray matter neurons, and ultimately influencing behaviors associated with neuropathic pain [24].

The abnormal mPFC responses, shared by cCH and eCH patients, associated with the attenuated VTA activity present only in cCH patients, may have two alternative explanations. The first is that altered top-down cortical influences from the mPFC may induce VTA dopaminergic dysfunctions. Although this possibility cannot be ruled out, the known pathophysiology of CH, in which a key role of the hypothalamus is hypothesized, together with the robust interactions between the VTA and the paraventricular nucleus [25], a hypothalamic nucleus involved in headache mechanisms [52] and anatomically abnormal (as part of the anterior-superior hypothalamic subunit) in patients with cCH [18], suggests a different interpretation. In fact, the second explanation is that the mPFC abnormal responses are driven by VTA dopaminergic dysfunctions, with the mPFC trying to compensate for those changes. Following this line of reasoning, it is possible to assume that while VTA dopaminergic dysfunctions may be fully established in cCH patients, abnormal mPFC responses in eCH patients might represent an early, albeit more subtle, sign of the VTA- dopaminergic system imbalance.

In this framework, abnormal VTA dopaminergic activity, in concert with the hypothalamus, could play a central role in inducing or modulating CH attacks and, only when severely impaired, lead to the chronic form of CH. This interpretation is strongly supported by empirical evidence that VTA-DBS can control attacks in severe forms of CH [3, 11].

Due to the possible confounding effects of medication-overuse headache (MOH), which can influence the activity of the mesocorticolimbic system [33], it is important to underline that although chronic CH patients may occasionally be at risk for medication overuse, none of the participants in our study met the clinical criteria for MOH, and all exhibited a distinct interictal period. As for the analgesic used to control the cluster headache attacks, all our patients employed subcutaneous Sumatriptan.

Conclusion

Our findings show a distinct involvement of the VTA in cCH and robustly indicate an imbalance of the VTA-mPFC pathways, supporting the hypothesis of an abnormal dopaminergic state in these patients. Although the picture is less clear for eCH patients, the observed mPFC alterations may represent an early sign of an emerging imbalance within the VTA-mPFC pathways. Remarkably, our results indicate an alteration in reward processing divergent from affective disorders, thus most likely indicating a mechanism underlying the pathophysiology of CH.

These findings are of fundamental importance for the development of future CH treatments, as they identify the mPFC and VTA as crucial targets for non-invasive therapeutic approaches. Targeting these areas holds significant potential for not only treating and preventing the chronification of this debilitating condition but also directly addressing acute attacks. The strong connections between VTA and mPFC, coupled with the extensive body of research on transcranial neurostimulation of prefrontal regions for neurological and psychiatric disorders, provide a solid foundation for implementing safe clinical trials aimed at restoring these pathways. Despite the complexity of managing cluster headache due to its variable clinical course and limited placebo-controlled evidence, advancing knowledge in neurobiology and emerging targeted therapies offer new hope for more effective and personalized preventive treatment strategies [45]. In light of our results, recent human studies indicate that compounds such as Oxytocin [22] and Losartan [64], which robustly interact with the dopaminergic system, can modulate VTA activity. In this framework, vagal nerve stimulation, shown to modulate VTA in animal models [10], has already demonstrated its efficacy in treating CH attacks [20, 43].

By leveraging our work and this existing knowledge, there is significant potential to develop innovative treatment strategies that could not only prevent chronic CH, but also provide effective relief from acute attacks.

Acknowledgements

We would like to thank our participants for generously taking part in this research. The Authors are grateful to the GARR consortium for the high-performance infrastructure used for the analyses at Neuroradiology Department of Fondazione IRCCS Istituto Neurologico Carlo Besta (Milan, Italy). We would like to thank the National Recovery and Resilience Plan (NRRP), Mission 4 Component 2 Investment 3.3 - Call for tender No. 117 of 02/03/2023 of the Italian Ministry of University and Research funded by the European Union– NextGenerationEU.

Author contributions

Authors contributions SF: conceptualization of the research, creation of the MIDT task, statistical analyses, interpretation of the data, major contributor in writing the manuscript, data collection; AN: conceptualization of the research, interpretation of the data, drafting the manuscript; MG, LC: conceptualization of the research, interpretation of the data, evaluation of the MRI data, drafting the manuscript; JPMC, BB, MM: interpretation of the data, drafting

the manuscript; DL, DF, GC: statistical analyses, interpretation of the data, drafting the manuscript; APC, LG, GDM, SU: conceptualization of the research, selection of the patients, data collection, clinical and demographic database, interpretation of the data; ML: conceptualization of the research, selection of the patients, interpretation of the data, major contributor in writing the manuscript. All authors read and approved the final manuscript.

Funding
This work was supported by the Key R&D Projects in Sichuan Province (research grant M112022YFWZ0003), the Italian Ministry of Health (research grant RF-2016-02364909, RRC), and the Fondazione Cariplo (research grant MESH 2022 – 0610).

Data availability
The data that support the findings of this study are not openly available due to reasons of sensitivity and are available from the corresponding author upon reasonable request. Data are located in controlled access data storage at the Neurological Institute Carlo Besta.

Declarations

Conflict of interest
The Authors report no conflict of interest.

Received: 13 January 2025 / Accepted: 30 March 2025
Published online: 19 May 2025

References

1. Abagnale C, Di Renzo A, Giuliani G, Sebastianelli G, Casillo F, Ziccardi L, Parisi V, Di Lorenzo C, Serrao M, Caramia F (2025) others. MRI-based analysis of the microstructure of the thalamus and hypothalamus and functional connectivity between cortical networks in episodic cluster headache. J Headache Pain 26:12
2. Absinta M, Rocca MA, Colombo B, Falini A, Comi G, Filippi M (2012) Selective decreased grey matter volume of the pain-matrix network in cluster headache. Cephalalgia 32:109–115
3. Akram H, Miller S, Lagrata S, Hyam J, Jahanshahi M, Hariz M, Matharu M, Zrinzo L (2016) Ventral tegmental area deep brain stimulation for refractory chronic cluster headache. Neurology 86:1676–1682
4. Apkarian AV (2004) Chronic back pain is associated with decreased prefrontal and thalamic Gray matter density. J Neurosci 24:10410–10415
5. Baker AK, Ericksen LC, Koppelmans V, Mickey BJ, Martucci KT, Zubieta J-K, Love TM (2022) Altered reward processing and sex differences in chronic pain. Front NeuroSci 16:889849
6. Baliki MN, Petre B, Torbey S, Herrmann KM, Huang L, Schnitzer TJ, Fields HL, Apkarian AV (2012) Corticostriatal functional connectivity predicts transition to chronic back pain. Nat Neurosci 15:1117–1119
7. Beck AT, Steer RA, Carbin MG (1988) Psychometric properties of the Beck depression inventory: Twenty-five years of evaluation. Clin Psychol Rev 8:77–100
8. Bjork JM, Grant SJ, Chen G, Hommer DW (2014) Dietary tyrosine/phenylalanine depletion effects on behavioral and brain signatures of human motivational processing. Neuropsychopharmacology 39:595–604
9. Bore MC, Liu X, Huang X, Kendrick KM, Zhou B, Zhang J, Klugah-Brown B, Becker B (2024) Common and separable neural alterations in adult and adolescent depression–evidence from neuroimaging meta-analyses. Neurosci Biobehavioral Reviews:105835
10. Brougher J, Aziz U, Adari N, Chaturvedi M, Jules A, Shah I, Syed S, Thorn CA (2021) Self-administration of right vagus nerve stimulation activates midbrain dopaminergic nuclei. Front NeuroSci 15:782786
11. Cheema S, Ferreira F, Parras O, Lagrata S, Kamourieh S, Pakzad A, Zrinzo L, Matharu M, Akram H (2023) Association of clinical and neuroanatomic factors with response to ventral tegmental area DBS in chronic cluster headache. Neurology 101:e2423–e2433
12. D'Andrea G, Granella F, Perini F, Farruggio A, Leone M, Bussone G (2006) Platelet levels of dopamine are increased in migraine and cluster headache. Headache: J Head Face Pain 46:585–591
13. D'Andrea G, Leone M, Bussone G, Fiore PD, Bolner A, Aguggia M, Saracco MG, Perini F, Giordano G, Gucciardi A, Leon A (2017) Abnormal tyrosine metabolism in chronic cluster headache. Cephalalgia 37:148–153
14. Demichelis G, Pinardi C, Giani L, Medina JP, Gianeri R, Bruzzone MG, Becker B, Proietti A, Leone M, Chiapparini L (eds) (2022);42:444–454
15. Feng C, Huang W, Xu K, Stewart JL, Camilleri JA, Yang X, Wei P, Gu R, Luo W, Eickhoff SB (2022) Neural substrates of motivational dysfunction across neuropsychiatric conditions: evidence from meta-analysis and lesion network mapping. Clin Psychol Rev 96:102189
16. Ferraro S, Medina JP, Nigri A, Giani L, Demichelis G, Pinardi C, Bruzzone MG, Cecchini Proietti A, Becker B, Chiapparini L (eds) (2022);42:1039–1049
17. Ferraro S, Nigri A, Bruzzone MG, Brivio L, Proietti Cecchini A, Verri M, Chiapparini L, Leone M (2018) Defective functional connectivity between posterior hypothalamus and regions of the diencephalic-mesencephalic junction in chronic cluster headache. Cephalalgia 38:1910–1918
18. Ferraro S, Nigri A, Bruzzone MG, Medina Carrion JP, Fedeli D, Demichelis G, Chiapparini L, Ciullo G, Gonzalez AA (2024) Proietti cecchini A, others. Involvement of the ipsilateral-to-the-pain anterior–superior hypothalamic subunit in chronic cluster headache. J Headache Pain 25:7
19. Galambos A, Szabó E, Nagy Z, Édes AE, Kocsel N, Juhász G, Kökönyei G (2019) A systematic review of structural and functional MRI studies on pain catastrophizing. J Pain Res 12:1155–1178
20. Gaul C, Diener H-C, Silver N, Magis D, Reuter U, Andersson A, Liebler EJ, Straube A (2016) Non-invasive vagus nerve stimulation for prevention and acute treatment of chronic cluster headache (PREVA): A randomised controlled study. Cephalalgia 36:534–546
21. Giorgio A, Lupi C, Zhang J, De Cesaris F, Alessandri M, Mortilla M, Federico A, Geppetti P, De Stefano N, Benemei S Changes in grey matter volume and functional connectivity in cluster headache versus migraine. Brain Imaging Behav 2019:1–9
22. Groppe SE, Gossen A, Rademacher L, Hahn A, Westphal L, Gründer G, Spreckelmeyer KN (2013) Oxytocin influences processing of socially relevant cues in the ventral tegmental area of the human brain. Biol Psychiatry 74:172–179
23. Hoffmann J, May A (2018) Diagnosis, pathophysiology, and management of cluster headache. Lancet Neurol 17:75–83
24. Huang S, Zhang Z, Gambeta E, Xu SC, Thomas C, Godfrey N, Chen L, M'Dahoma S, Borgland SL, Zamponi GW (2020) Dopamine inputs from the ventral tegmental area into the medial prefrontal cortex modulate neuropathic pain-associated behaviors in mice. Cell Rep;31
25. Hung LW, Neuner S, Polepalli JS, Beier KT, Wright M, Walsh JJ, Lewis EM, Luo L, Deisseroth K, Dölen G, Malenka RC (2017) Gating of social reward by Oxytocin in the ventral tegmental area. Science 357:1406–1411
26. Kim M, Mawla I, Albrecht DS, Admon R, Torrado-Carvajal A, Bergan C, Protsenko E, Kumar P, Edwards RR (2020) Saha A, others. Striatal hypofunction as a neural correlate of mood alterations in chronic pain patients. Neuroimage 211:116656
27. Knutson B, Bhanji JP, Cooney RE, Atlas LY, Gotlib IH (2008) Neural responses to monetary incentives in major depression. Biol Psychiatry 63:686–692
28. Knutson B, Bjork JM, Fong GW, Hommer D, Mattay VS, Weinberger DR (2004) Amphetamine modulates human incentive processing. Neuron 43:261–269
29. Knutson B, Heinz A (2015) Probing psychiatric symptoms with the monetary incentive delay task. Biol Psychiatry 77:418–420
30. Knutson B, Taylor J, Kaufman M, Peterson R, Glover G (2005) Distributed neural representation of expected value. J Neurosci 25:4806–4812
31. Knutson B, Westdorp A, Kaiser E, Hommer D (2000) FMRI visualization of brain activity during a monetary incentive delay task. NeuroImage 12:20–27
32. Kocsel N, Galambos A, Szabó E, Édes AE, Magyar M, Zsombók T, Pap D, Kozák LR, Bagdy G, Kökönyei G (2019) others. Altered neural activity to monetary reward/loss processing in episodic migraine. Sci Rep 9:5420
33. Lai T-H, Wang S-J (2018) Neuroimaging findings in patients with medication overuse headache. Curr Pain Headache Rep 22:1–7
34. Lammel S, Hetzel A, Häckel O, Jones I, Liss B, Roeper J (2008) Unique properties of mesoprefrontal neurons within a dual mesocorticolimbic dopamine system. Neuron 57:760–773
35. Martucci KT, Borg N, MacNiven KH, Knutson B, Mackey SC (2018) Altered prefrontal correlates of monetary anticipation and outcome in chronic pain. Pain 159:1494–1507
36. Matharu MS, Zrinzo L (2010) Deep brain stimulation in cluster headache: hypothalamus or midbrain tegmentum? Curr Pain Headache Rep 14:151–159
37. Matos SC, Zhang Z, Séguéla P (2015) Peripheral neuropathy induces HCN channel dysfunction in pyramidal neurons of the medial prefrontal cortex. J Neurosci 35:13244–13256

38. May A, Bahra A, Büchel C, Frackowiak RSJ, Goadsby PJ (1998) Hypothalamic activation in cluster headache attacks. Lancet 352:275–278
39. Metz AE, Yau H-J, Centeno MV, Apkarian AV, Martina M (2009) Morphological and functional reorganization of rat medial prefrontal cortex in neuropathic pain. Proceedings of the National Academy of Sciences.;106:2423–2428
40. Mohebi A, Pettibone JR, Hamid AA, Wong J-MT, Vinson LT, Patriarchi T, Tian L, Kennedy RT, Berke JD (2019) Dissociable dopamine dynamics for learning and motivation. Nature 570:65–70
41. Moriarty O, McGuire BE, Finn DP (2011) The effect of pain on cognitive function: a review of clinical and preclinical research. Prog Neurobiol 93:385–404
42. Naegel S, Holle D, Desmarattes N, Theysohn N, Diener H-C, Katsarava Z, Obermann M (2014) Cortical plasticity in episodic and chronic cluster headache. NeuroImage: Clin 6:415–423
43. Nesbitt AD, Marin JCA, Tompkins E, Ruttledge MH, Goadsby PJ (2015) Initial use of a novel noninvasive vagus nerve stimulator for cluster headache treatment. Neurology 84:1249–1253
44. Olesen J (2018) Headache classification committee of the international headache society (IHS) the international classification of headache disorders. Cephalalgia 38:1–211
45. Orvin CA, Zaheri SC, Perilloux DM, Field E, Ahmadzadeh S, Shekoohi S, Kaye AD, Divalproex (2024) Valproate, & developing treatment options for cluster headache prophylaxis: clinical practice considerations. SN Compr Clin Med 6:16
46. Ott T, Nieder A (2019) Dopamine and cognitive control in prefrontal cortex. Trends Cogn Sci 23:213–234
47. Park SH, Deng EZ, Baker AK, MacNiven KH, Knutson B, Martucci KT (2022) Altered brain reward response to monetary incentives in fibromyalgia: A replication study. MedRxiv:2022–2003
48. Pauli WM, Nili AN, Tyszka JM (2018) A high-resolution probabilistic in vivo atlas of human subcortical brain nuclei. Sci Data 5:1–13
49. Popescu AT, Zhou MR, Poo M (2016) Phasic dopamine release in the medial prefrontal cortex enhances stimulus discrimination. Proceedings of the National Academy of Sciences.;113:E3169–E3176
50. Power JD, Barnes KA, Snyder AZ, Schlaggar BL, Petersen SE (2012) Spurious but systematic correlations in functional connectivity MRI networks arise from subject motion. NeuroImage 59:2142–2154
51. Ranganathan P, Pramesh C, Aggarwal R (2017) Common pitfalls in statistical analysis: logistic regression. Perspect Clin Res 8:148–151
52. Roberts MJ, Lowet E, Brunet NM, TerWal M, Tiesinga P, Fries P, DeWeerd P (2013) Robust gamma coherence between macaque V1 and V2 by dynamic frequency matching. Neuron 78:523–536
53. Rocca MA, Valsasina P, Absinta M, Colombo B, Barcella V, Falini A, Comi G, Filippi M (2010) Central nervous system dysregulation extends beyond the pain-matrix network in cluster headache. Cephalalgia 30:1383–1391
54. Russo SJ, Nestler EJ (2014) The brain reward circuitry in mood disorders. Nat Rev Neurosci 14:609–625
55. Schott BH, Minuzzi L, Krebs M, Elmenhorst D, Lang M, Winz O, Seidenbecher CI, Coenen H, Heinze H-J, Zilles K (2008) others. Mesolimbic fMRI activations during reward anticipation correlate with reward-related ventral striatal dopamine release. J Neurosci 28:14311–14319
56. Serafini RA, Pryce KD, Zachariou V (2020) The mesolimbic dopamine system in chronic pain and associated affective comorbidities. Biol Psychiatry 87:64–73
57. Spielberger CD (1970) Manual for the State-Trait Anxiety Inventory (self-evaluation questionnaire). (No Title)
58. Taylor NE, Van Doort C, Kenny J, Pei J, Huidera J, Vlasov K, Lee J, Boyden E, Brown E, Solt K (2016) Optogenetic activation of dopamine neurons in the ventral tegmental area induces reanimation from general anesthesia. PNAS 113:12825–12831
59. Vachon-Presseau E, Centeno M, Ren W, Berger S, Tétreault P, Ghantous M, Baria A, Farmer M, Baliki M, Schnitzer T, others (2016) The emotional brain as a predictor and amplifier of chronic pain. J Dent Res 95:605–612
60. Vachon-Presseau E, Tétreault P, Petre B, Huang L, Berger SE, Torbey S, Baria AT, Mansour AR, Hashmi JA, Griffith JW (2016) others. Corticolimbic anatomical characteristics predetermine risk for chronic pain. Brain 139:1958–1970
61. Vittinghoff E, McCulloch CE (2007) Relaxing the rule of ten events per variable in logistic and Cox regression. Am J Epidemiol 165:710–718
62. Walfish S (2006) A review of statistical outlier methods. Pharm Technol 30:82
63. West RM (2022) Best practice in statistics: the use of log transformation. Ann Clin Biochem 59:162–165
64. Zhou X, Xu T, Zeng Y, Zhang R, Qi Z, Zhao W, Kendrick KM, Becker B (2023) The angiotensin antagonist Losartan modulates social reward motivation and punishment sensitivity via modulating midbrain-striato-frontal circuits. J Neurosci 43:472–483

Publisher's note